

## Reply to report #1

Thank you for your comments.

The authors have incorporated most of the comments of the reviewers, and paper now is greatly improved with the incorporation of salinity, temperature, Chl a and NH<sub>4</sub>. I commend the authors on their efforts, and find that they have responded appropriately to the reviews. I had just a few minor comments for consideration.

Lines 130-131: I agree with the authors that sample date should be adjusted to a regular spacing. However, I do not agree with the assumption of no not temporal variability between weeks. The authors should use a lineal interpolation (or test other models) to homogenize dates, or in lack of this, demonstrate that the uncertainty introduced with such assumption is not significant.

We used a linear interpolation to homogenize the dates and found a overall error of 4.2%. In this case, we modified the text into “Sampling time varied for every month (usually 20-40 day interval), but for the statistical analysis, data was assumed to be regularly spaced as the uncertainty introduced was not significant (<5%).”

Lines 238-239: The authors should include a reference for the O<sub>2</sub> limit used for the inhibition of denitrification.

According to Tiedje (1988), we included the O<sub>2</sub> threshold of ~10 μmol L<sup>-1</sup> for the inhibition of denitrification.

The following changes have been made in the manuscript:

1. Include the uncertainty introduced from the date shift in line 131.
2. Include the O<sub>2</sub> threshold for the inhibition of denitrification in lines 240–241.
3. Add a reference in lines 651–653.

# A multi-year observation of nitrous oxide at the Boknis Eck Time-Series Station in the Eckernförde Bay (southwestern Baltic Sea)

Xiao Ma<sup>1</sup>, Sinikka T. Lennartz<sup>1,2</sup>, and Hermann W. Bange<sup>1</sup>

<sup>1</sup> GEOMAR Helmholtz Centre for Ocean Research Kiel, Düsternbrooker Weg 20, 24105 Kiel, Germany

<sup>2</sup> now at ICBM, University of Oldenburg, Oldenburg, Germany

*Correspondence to:* Xiao Ma (mxiao@geomar.de)

**Abstract.** Nitrous oxide (N<sub>2</sub>O) is a potent greenhouse gas and it is involved in stratospheric ozone depletion. Its oceanic production is mainly influenced by dissolved nutrient and oxygen (O<sub>2</sub>) concentrations in the water column. Here we examined the seasonal and annual variations of dissolved N<sub>2</sub>O at the Boknis Eck (BE) Time-Series Station located in Eckernförde Bay (southwestern Baltic Sea). Monthly measurements of N<sub>2</sub>O started in July 2005. We found a pronounced seasonal pattern for N<sub>2</sub>O with high concentrations (supersaturations) in winter/early spring and low concentrations (undersaturations) in autumn when hypoxic/anoxic conditions prevail. Unusually low N<sub>2</sub>O concentrations were observed during October 2016–April 2017, which was presumably a result of prolonged anoxia and the subsequent nutrient deficiency. Unusually high N<sub>2</sub>O concentrations were found in November 2017 and this event was linked to the occurrence of upwelling which interrupted N<sub>2</sub>O consumption via denitrification and potentially promoted ammonium oxidation (nitrification) at the oxic/anoxic interface. Nutrient concentrations (such as nitrate, nitrite and phosphate) at BE are decreasing since 1980s, but oxygen concentrations in the water column are still decreasing. Our results indicate a close coupling of N<sub>2</sub>O anomalies to O<sub>2</sub> concentration, nutrients and stratification. Given the long-term trends of declining nutrient and oxygen concentrations at BE, a decrease in N<sub>2</sub>O concentration, and thus emissions, seems likely due to an increasing number of events with low N<sub>2</sub>O concentrations.

## 1. Introduction

Long-term observation with regular measurement intervals can be an effective way to monitor seasonal and interannual variabilities as well as to decipher short- and long-term trends of an ecosystem, which are required to make projections of the future ecosystem development (see e.g. Ducklow et al., 2009). Recently, multi-year time-series measurements of nitrous oxide (N<sub>2</sub>O), a potent greenhouse gas and a major threat to ozone depletion (IPCC, 2013; Ravishankara et al., 2009), have been reported from the coastal upwelling areas off central Chile (Farías et al., 2015) and off Goa (Naqvi et al., 2010), in the North Pacific Subtropical Gyre (Wilson et al., 2017), and in Saanich Inlet (Capelle et al., 2018).

36 N<sub>2</sub>O production in the ocean is generally dominated by microbial nitrification (NH<sub>4</sub><sup>+</sup> → NO<sub>2</sub><sup>-</sup> →  
37 NO<sub>3</sub><sup>-</sup>) and denitrification (NO<sub>3</sub><sup>-</sup> → NO<sub>2</sub><sup>-</sup> → N<sub>2</sub>O → N<sub>2</sub>). During bacterial/archaeal nitrification,  
38 N<sub>2</sub>O is produced as a by-product with enhanced N<sub>2</sub>O production under low oxygen (O<sub>2</sub>)  
39 conditions (e.g. Goreau et al., 1980; Löscher et al., 2012). N<sub>2</sub>O is produced as an intermediate  
40 during bacterial denitrification (Codispoti et al., 2005). N<sub>2</sub>O could be further consumed via  
41 denitrification to dinitrogen, however, this process is inhibited with the presence of O<sub>2</sub> because  
42 of the low O<sub>2</sub> tolerance of the enzyme involved (Bonin et al. 1989). This incomplete pathway is  
43 called partial denitrification and can lead to N<sub>2</sub>O accumulation (e.g. Naqvi et al., 2000; Farías et  
44 al., 2009).

45 The oceans including coastal areas contribute ~25% of the natural and anthropogenic N<sub>2</sub>O  
46 emissions (IPCC, 2013), with disproportionately high emissions from coastal and estuarine areas  
47 (Bange, 2006). N<sub>2</sub>O emissions from coastal areas strongly depend on nitrogen inputs (Seitzinger  
48 and Kroeze, 1998; Zhang et al., 2010). The increasing input of nitrogen (i.e. eutrophication) has  
49 become a worldwide problem in coastal waters leading to enhanced productivity and severe O<sub>2</sub>  
50 depletion caused by enhanced degradation of organic matter (Breitburg et al., 2018; Rabalais et  
51 al., 2014). The decline in O<sub>2</sub> concentration (i.e. deoxygenation), either in coastal waters or the  
52 open ocean, might result in favorable conditions for N<sub>2</sub>O production (Codispoti et al., 2001;  
53 Nevison et al., 2003). The results of a model study by Kroeze and Seitzinger (1998) indicated a  
54 significant increase of N<sub>2</sub>O in European coastal waters for 2050. Moreover, it has been suggested  
55 that N<sub>2</sub>O production and emissions are very likely to increase in the near future, especially in the  
56 shallow suboxic/anoxic coastal systems (Naqvi et al., 2000; Bange, 2006). However, model  
57 projections show a net decrease in future global oceanic N<sub>2</sub>O emission during the 21<sup>st</sup> century  
58 (Martinez-Rey et al., 2015; Landolfi et al., 2017; Battaglia and Joos, 2018).

59 The Baltic Sea is a nearly enclosed, marginal sea with a very limited access to the open ocean via  
60 the North Sea. The restricted water exchange with the North Sea and extensive human activities,  
61 such agriculture, industrial production and sewage discharge in the catchment area led to high  
62 inputs of nutrients to the Baltic Sea. As a result, the areas affected by anoxia have been  
63 expanding in the deep basins of the central Baltic Sea (Carstensen et al., 2014). In order to  
64 control this situation, the Helsinki Commission (HELCOM) was established in 1974 and a series  
65 of measures have been taken to prevent anthropogenic nutrient input into the Baltic Sea.  
66 Consequently, the nutrient inputs (by riverine loads, direct point-sources and, for nitrogen,  
67 atmospheric deposition) to the Baltic Sea are declining (HELCOM, 2018a). However, the  
68 number of low O<sub>2</sub> (i.e. hypoxic/anoxic) events in coastal waters of the Baltic Sea is increasing  
69 and deoxygenation is still going on (Conley et al., 2011; Lennartz et al., 2014). The  
70 deoxygenation in the Baltic Sea can affect the production/consumption of N<sub>2</sub>O. Our group has  
71 been monitoring dissolved N<sub>2</sub>O concentrations at the Boknis Eck Time-Series Station, located in  
72 Eckernförde Bay (southwestern Baltic Sea), for more than a decade. In this study, we present  
73 monthly measurements of N<sub>2</sub>O and biogeochemical parameters such as nutrients and O<sub>2</sub> from  
74 July 2005 to December 2017. The major objectives of our study were: 1) to decipher the seasonal

75 pattern of N<sub>2</sub>O distribution in the water column, 2) to identify short-term and long-term trends of  
76 the N<sub>2</sub>O concentrations, 3) to explore the potential role of nutrients and O<sub>2</sub> for N<sub>2</sub>O  
77 production/consumption, and 4) to quantify the sea-to-air N<sub>2</sub>O flux density at the time-series  
78 station.

## 79 **2. Material and methods**

### 80 **2.1 Study site**

81 Sampling at the Boknis Eck (BE) Time-Series Station ([www.bokniseck.de](http://www.bokniseck.de)) started on 30 April  
82 1957 and, therefore, it is one of the oldest continuously operated time-series stations in the world.  
83 The BE station is located at the entrance of the Eckernförde Bay (54°31' N, 10°02' E, Fig. 1) in  
84 the southwestern Baltic Sea. The water depth of the sampling site is 28 m. Various physical,  
85 chemical and biological parameters are measured on a monthly basis (Lennartz et al., 2014).  
86 There is no significant river runoff to Eckernförde Bay. Hence, the hydrographical conditions are  
87 mainly dominated by saline water input from the North Sea and less saline water from the Baltic  
88 Proper, which is typical for that region. Seasonal stratification usually starts to develop in April  
89 and lasts until October, during which hypoxia or even anoxia (characterized by the presence of  
90 hydrogen sulphide, H<sub>2</sub>S) sporadically occurs, as a result of restricted vertical water exchange and  
91 bacterial decomposition of organic matter in the bottom water (Hansen et al., 1999; Lennartz et  
92 al., 2014). Thus, BE is a natural laboratory to study the influence of O<sub>2</sub> variations and  
93 anthropogenic nutrient loads on N<sub>2</sub>O production/consumption.

### 94 **2.2 Sample collection and measurement**

95 Monthly sampling of N<sub>2</sub>O at the BE Time-Series Station started in July 2005. Triplicate samples  
96 were collected from six depths (1, 5, 10, 15, 20 and 25 m). Seawater was drawn from 5 L Niskin  
97 bottles into 20 mL brown glass vials after overflow. The vials were sealed with rubber stoppers  
98 and aluminum caps. The bubble-free samples were poisoned with 50 µL of a saturated mercury  
99 chloride (HgCl<sub>2</sub>) solution and then stored in a cool, dark place until measurement. The general  
100 storage time before measurements of the N<sub>2</sub>O concentrations was less than three months.

101 The static headspace-equilibrium method was adopted to measure the dissolved N<sub>2</sub>O  
102 concentrations in the vials. 10 mL helium (99.9999 %, AirLiquide, Düsseldorf, Germany)  
103 headspace was created in each vial with a gas-tight glass syringe (VICI Precision Sampling,  
104 Baton Rouge, LA). Samples were vibrated with Vortex (G-560E, Scientific Industries Inc., New  
105 York, USA) for 20 seconds and then left for at least two hours until equilibrium. 9.5 mL  
106 subsample of the headspace was subsequently injected into a GC-ECD (gas chromatograph  
107 equipped with the electron capture detector) system (Hewlett-Packard 5890 Series II, Agilent  
108 Technologies, Santa Clara, CA, USA), which was calibrated with two standard gas mixtures  
109 (N<sub>2</sub>O in synthetic air, 320 ppb and 1000 ppb, Deuste-Steininger GmbH, Mühlhausen, Germany  
110 and Westfalen AG, Münster, Germany) prior to the measurement. The average precision of the

111 measurements, calculated as the median standard deviation from triplicate measurements, was  
112 0.4 nM. Triplicates with a standard deviation of >10% were omitted. More details about the N<sub>2</sub>O  
113 measurement can be found in Kock et al. (2016). Dissolved oxygen (O<sub>2</sub>) concentrations were  
114 measured by Winkler titrations (Grasshoff et al., 1999). Nutrient concentrations were measured  
115 by the Segmented Continuous Flow Analysis (SCFA, Grasshoff et al., 1999). A more detailed  
116 summary of the parameters measured and methods applied can be found in Lennartz et al. (2014).

## 117 **2.3 Times series analysis**

118 A time-series can be decomposed into three main components, i.e. trend, cycle and residual  
119 component (Schlittgen and Streitberg, 2001). We used the Mann–Kendall test and wavelet  
120 analysis to detect the trend and periodical cycles in the time-series data, respectively. As for the  
121 residual component, we highlight unusual high/low N<sub>2</sub>O concentrations during 2005-2017 and  
122 discuss the potential causes for these events.

### 123 **2.3.1 Wavelet analysis**

124 In order to decipher periodical cycles of the parameters collected at the BE Time-Series Station,  
125 a wavelet analysis method was adopted. Wavelet analysis enables the detection of the period and  
126 the temporal occurrence of repeated cycles in time-series data. One of the requirements for  
127 wavelet analysis is a regular, continuous time-series. Since there is data missing (maximum 2  
128 months in a row) in the BE time-series, due to terrible weather or the ship's unavailability,  
129 missing data was interpolated from the previous and following months. Sampling time varied for  
130 every month (usually 20-40 day interval), but for the statistical analysis, data was assumed to be  
131 regularly spaced as **the uncertainty introduced was not significant (<5%)**. Considering the band  
132 width in both frequency and time domain, a Morlet mother wavelet with a wave number of 6 was  
133 chosen (Torrence and Compo, 1998). The mother wavelet was then scaled between the  
134 frequency of a half-year cycle and the length of the time-series with a stepsize of 0.25. The  
135 wavelet analysis was conducted with the MatLab code by Torrence and Compo [2004]. More  
136 information about the method can be found on the website  
137 <http://paos.colorado.edu/research/wavelets/>.

### 138 **2.3.2 Mann–Kendall test**

139 Mann–Kendall test (MKT) is a non-parametric statistical test to assess the significance of  
140 monotonic trends for time-series measurements. It tests the null hypothesis that all variables are  
141 randomly distributed against the alternative hypothesis that a monotonic trend, either increase or  
142 decrease, exists in the time-series on a given significance level  $\alpha$  (here  $\alpha=0.05$ ). MKT is flexible  
143 for data with missing values and the results are not impacted by the magnitude of extreme values,  
144 which makes it a widely used test in hydrology and climatology (e.g. Xu et al., 2003; Yang et al.,  
145 2004). However, MKT is sensitive to serial correlation in the time-series. The presence of  
146 positive serial correlation would increase the probability of trend detection even though no such

147 trend exists (Kulkarni and von Storch, 1995). In order to avoid this situation, data from 12  
148 months were tested individually. It is assumed that there is no residual effect left from the same  
149 month last year, considering that the nitrogen species are rapidly biologically cycled. The Matlab  
150 function from Simone (2009) was used for the MKT.

## 151 **2.4 Calculation of saturation and sea-to-air flux density**

152 N<sub>2</sub>O saturations ( $S_{N_2O}$ , %) were calculated as:

$$153 \quad S_{N_2O} = 100 \times N_{2O_{obs}}/N_{2O_{eq}} \quad (1)$$

154 where  $N_{2O_{obs}}$  and  $N_{2O_{eq}}$  (in nM) are the observed and equilibrated N<sub>2</sub>O concentrations in  
155 seawater, respectively.  $N_{2O_{eq}}$  was computed as a function of surface seawater temperature, in  
156 situ salinity (Weiss and Price, 1980) and the dry mole fractions of atmospheric N<sub>2</sub>O at the time  
157 of the sampling. Since the atmospheric N<sub>2</sub>O mole fractions were not measured at the BE Time-  
158 Series Station, atmospheric dry mole fractions of N<sub>2</sub>O were derived from the monthly average of  
159 N<sub>2</sub>O data at Mace Head, Ireland (AGAGE, <http://agage.mit.edu/>), instead.

160 N<sub>2</sub>O flux density ( $F_{N_2O}$ , in  $\mu\text{mol m}^{-2} \text{d}^{-1}$ ) was calculated as:

$$161 \quad F_{N_2O} = k_{N_2O} \times (N_{2O_{obs}} - N_{2O_{eq}}) \quad (2)$$

162 where  $k_{N_2O}$  (in  $\text{cm h}^{-1}$ ) is the gas transfer velocity calculated with the method given by  
163 Nightingale et al. (2000), as a function of the wind speed and the Schmidt number ( $Sc$ ). The wind  
164 speed data were obtained from the Kiel Lighthouse (see: [www.geomar.de/service/wetter/](http://www.geomar.de/service/wetter/)), which  
165 is approximately 20 km away from the BE Time-Series Station. The wind speed was normalized  
166 to 10 m ( $u_{10}$ ) to calculate  $k_{N_2O}$  (Hsu et al., 1994).  $k_{N_2O}$  was adjusted by multiplying with  $(Sc/600)^{0.5}$ ,  
167 and  $Sc$  was computed as:

$$168 \quad Sc = \nu/D_{N_2O} \quad (3)$$

$$169 \quad D_{N_2O} = 3.16 \times 10^{-6} e^{-18370/RT} \quad (4)$$

170 where  $\nu$  is the kinematic viscosity of seawater, which is calculated from the empirical equations  
171 given in Siedler and Peters (1986), and  $D_{N_2O}$  is the diffusion coefficient of N<sub>2</sub>O in seawater.  $R$  is  
172 the universal gas constant and  $T$  is the water temperature in K.

## 173 **3. Result and discussion**

### 174 **3.1 Overview**

175 N<sub>2</sub>O concentrations at the BE Time-Series Station showed significant temporal and depth-  
176 dependent variations from 2005 to 2017 (Fig. 2). N<sub>2</sub>O concentrations fluctuated between 1.2 and  
177 37.8 nM, with an overall average of  $13.9 \pm 4.2$  nM. This value was higher than the results from

178 the surface water of Station ALOHA ( $5.9\text{--}7.4\text{ nmol kg}^{-1}$ , average  $6.5\pm 0.3\text{ nmol kg}^{-1}$ , Wilson et  
179 al., 2017), which is reasonable considering the weak anthropogenic impact in the North Pacific  
180 Subtropical Gyre. The  $\text{N}_2\text{O}$  concentrations at BE were much lower than those measured at the  
181 time-series station in the coastal upwelling area off Chile ( $2.9\text{--}492\text{ nM}$ , average  $39.4\pm 29.2\text{ nM}$  in  
182 the oxyclines and  $37.6\pm 23.3\text{ nM}$  in the bottom waters, Farías et al., 2015) and a quasi-time series  
183 station off Goa (Naqvi et al., 2010), where significant  $\text{N}_2\text{O}$  accumulations were observed in  
184 subsurface waters at both locations. Our measurements were comparable to the time-series  
185 station from Saanich Inlet ( $\sim 0.5\text{--}37.4\text{ nM}$ , average  $14.7\text{ nM}$ , Capelle et al., 2018), a seasonally  
186 anoxic fjord which has similar hydrographic conditions as BE.

187  $\text{NO}_2^-$  concentrations fluctuated between below detection limit of  $0.1\text{ }\mu\text{M}$  and  $1.6\text{ }\mu\text{M}$ , with an  
188 average of  $0.2\pm 0.3\text{ }\mu\text{M}$ .  $\text{NO}_3^-$  concentrations varied from below detection limit of  $0.3\text{ }\mu\text{M}$  to  $17.9$   
189  $\mu\text{M}$ , with an average of  $2.0\pm 2.8\text{ }\mu\text{M}$ . The temporal and spatial distributions of nitrite ( $\text{NO}_2^-$ ) and  
190 nitrate ( $\text{NO}_3^-$ ) were similar during 2005–2017. A clear  $\text{O}_2$  seasonality can be seen with severe  $\text{O}_2$   
191 depletion in the bottom waters during summer and autumn. Anoxia with the presence of  $\text{H}_2\text{S}$   
192 were detected in September/October 2005, September 2007, September/October 2014, and  
193 September–November 2016. All of the extremely low  $\text{N}_2\text{O}$  concentrations ( $<5\text{ nM}$ ) were  
194 observed in the bottom waters in autumn, coinciding with hypoxia/anoxia, while the high  $\text{N}_2\text{O}$   
195 concentrations ( $>20\text{ nM}$ ) sporadically occurred at different depths either in spring or autumn.

### 196 **3.2 Seasonal cycle**

197 Significant cycles at different frequencies were detected via wavelet analysis at the BE Time-  
198 Series Station during 2005–2017 (Fig. 3). A half-year  $\text{NO}_2^-$  cycle sporadically occurred in 2007–  
199 2009, 2013 and 2015. There is a seasonal  $\text{NO}_2^-$  variability (at the frequency of 1 year) between  
200 2007 and 2016 (times before 2007 and after 2016 were outside the conic line), except during  
201 2010–2012, when high  $\text{NO}_2^-$  concentrations were not observed in winter (Fig. 2). A biennial  
202 cycle of  $\text{NO}_2^-$  could be observed as well during 2008–2015. The  $\text{NO}_3^-$  concentrations were  
203 dominated by an annual cycle and a minor half-year cycle. The biennial cycle only occurred in  
204 2008 and 2009. A remarkable seasonal variability of dissolved  $\text{O}_2$  prevailed all the time, which is  
205 also obvious from the times series data shown in Fig. 2. The annual  $\text{N}_2\text{O}$  cycle became gradually  
206 more and more evident until 2014, then declined and reoccurred less intensely in 2016. The  
207 periodical cycle was also present at other frequencies, indicated by the broadening of the red area  
208 before 2015 in Fig. 2d. For example, a biennial  $\text{N}_2\text{O}$  cycle occurred during 2013–2015.

209 The half-year cycles of  $\text{NO}_2^-$  and  $\text{NO}_3^-$  were probably associated with algae blooms which  
210 usually occur in each spring and autumn (Fig. S1 and S2). Since the time between the two  
211 blooms differed between years, the cycles were weak and thus not present in every year. Due to  
212 the fact that there was no half-year  $\text{O}_2$  cycle at all, nutrients apart from  $\text{O}_2$  might be the “drivers”  
213 of the sporadic half-year  $\text{N}_2\text{O}$  cycle in 2008 and 2015, because  $\text{N}_2\text{O}$  production depends on the  
214 concentration of the bioavailable nitrogen compounds (Codispoti et al., 2001).



215 Generally the wavelet analysis indicated a strong annual cycle for  $\text{NO}_2^-$ ,  $\text{NO}_3^-$ , dissolved  $\text{O}_2$  and  
216  $\text{N}_2\text{O}$  at the BE Time-Series Station, which enabled us to explore the seasonal pattern with annual  
217 mean data. Although extreme values were excluded as a result of averaging, the smoothed results  
218 generally reflect the seasonality of these parameters. Here, we focus on the annual cycle.

219 The annual mean vertical distribution of dissolved  $\text{O}_2$ ,  $\text{NO}_2^-$ ,  $\text{NO}_3^-$  and  $\text{N}_2\text{O}$  are shown in Fig. 4.  
220 Due to the development of stratification, the mixed layer was shallow in summer and deep in late  
221 autumn/winter.  $\text{O}_2$  depletion was observed in bottom waters from late spring until late autumn.  
222 The seasonal variations of  $\text{NO}_2^-$  and  $\text{NO}_3^-$  were significantly correlated with each other  
223 ( $[\text{NO}_3^-]=11.59[\text{NO}_2^-]-0.51$ ,  $R^2=0.80$ ,  $n=72$ ,  $p<0.0001$ ) and high concentrations were observed  
224 for both in winter. Minimum  $\text{N}_2\text{O}$  concentrations were found in the bottom waters during  
225 September and October, presumably as a result of consumption during denitrification under  
226 anoxic condition (Codispoti et al., 2005). High  $\text{N}_2\text{O}$  concentrations were observed in late spring  
227 and late autumn, respectively. In late spring  $\text{N}_2\text{O}$  accumulated in the bottom waters because the  
228 stratification prevented mixing of the water column. In late autumn, however,  $\text{N}_2\text{O}$  could be  
229 ventilated to the surface and thus emitted to the atmosphere due to the breakdown of the  
230 stratification. The high  $\text{N}_2\text{O}$  concentrations could be attributed to enhanced  $\text{N}_2\text{O}$  production via  
231 nitrification and/or denitrification within the oxic/anoxic interface (Goreau et al., 1980;  
232 Codispoti et al., 1992). Since there is no clear  $\text{O}_2$  concentration threshold,  $\text{N}_2\text{O}$  production from  
233 both nitrification and the onset of denitrification overlap at oxic/anoxic interface. To this end,  
234 direct  $\text{N}_2\text{O}$  production measurements (i.e. nitrification/denitrification rates) are required to  
235 decipher which process dominates the formation of the different  $\text{N}_2\text{O}$  maxima.

236 High  $\text{N}_2\text{O}$  concentrations prevailed all over the water column in winter/early spring.  $\text{NH}_4^+$  is  
237 released from the sediment into bottom waters due to the degradation of organic matter,  
238 especially after the autumn algae bloom (Fig. S1 and S2). The stratification usually completely  
239 breaks down at this time of the year and the water column becomes oxygenated. Denitrification  
240 is inhibited by the presence of high concentrations of dissolved  $\text{O}_2$  ( $> 20 \mu\text{mol L}^{-1}$ , which is  
241 higher than the  $\text{O}_2$  threshold of about  $10 \mu\text{mol L}^{-1}$ , Tiedje, 1988) and thus nitrification is  
242 presumably responsible for the high  $\text{N}_2\text{O}$  concentrations in winter/early spring.

### 243 3.3 Trend analysis

244 The MKTs were conducted for the surface (1m) and bottom (25m)  $\text{N}_2\text{O}$  concentrations and  
245 saturations of the individual 12 months, respectively. Significant decreasing trends were detected  
246 for the concentrations in the bottom waters for February and August (Table 1a), and for the  
247 saturations in the surface for September and in the bottom for August and November (Table 1b).  
248 These results indicated that some systematical changes in  $\text{N}_2\text{O}$  took place at BE. For example,  
249 the significant decrease in  $\text{N}_2\text{O}$  concentration/saturation in August might be associated with the  
250 increasing temperature, which reinforces the stratification and accelerates  $\text{O}_2$  consumption in the  
251 bottom waters (Lennartz et al., 2014). As a result, hypoxia/anoxia starts earlier and thus enables

252 the onset of denitrification to consume N<sub>2</sub>O. During most of the months, trends in N<sub>2</sub>O  
253 concentration and saturation were not significant during 2005–2017.

254 A significant nutrient decline has been observed at the BE Time-Series Station since the mid-  
255 1980s, however, Lennartz et al. (2014) found that bottom O<sub>2</sub> concentrations were still decreasing  
256 over the past 60 years. The ongoing oxygen decline was attributed to the temperature-enhanced  
257 O<sub>2</sub> consumption in the bottom water (Meier et al., 2018) and a prolongation of the stratification  
258 period at the BE Time-Series Station (Lennartz et al., 2014). Please note that the trends in  
259 nutrients and O<sub>2</sub> concentrations were detected based on the data collection which lasted for  
260 approximately 30 and 60 years, respectively, while the N<sub>2</sub>O observations at BE Time-Series  
261 Station has lasted for only 12.5 years. Further MKT analysis for nutrients, temperature and  
262 oxygen for months with significant trends in N<sub>2</sub>O concentrations did not show any significant  
263 results ( $p>0.05$ ). The significant trends in N<sub>2</sub>O concentrations thus do not seem to be directly  
264 related to one of these parameters, and we cannot state a reason for the significant trends of N<sub>2</sub>O  
265 concentration in February and the N<sub>2</sub>O saturation in September and November at this point.  
266 Presumably, a longer monitoring period for N<sub>2</sub>O is required to detect corresponding trends in  
267 N<sub>2</sub>O and oxygen or nutrients.

## 268 **3.4 Extreme events**

### 269 **3.4.1 Low N<sub>2</sub>O concentrations during October 2016-April 2017**

270 Besides the low N<sub>2</sub>O concentrations occurring in autumn, we observed a band of pronounced  
271 low N<sub>2</sub>O concentrations which started in October 2016 and lasted until April 2017 (Fig. 5). In  
272 this period N<sub>2</sub>O concentrations varied between 5.5–13.9 nM, with an average of  $8.4\pm 2.0$  nM.  
273 This is approximately 40% lower than the average N<sub>2</sub>O concentration during the entire  
274 measurement period 2005–2017. The average N<sub>2</sub>O saturation during 2005–2017 was  $111\pm 30\%$ ,  
275 while from October 2016 to April 2017, the N<sub>2</sub>O saturations were as low as 43–93% (average  
276  $62\pm 10\%$ ).

277 Undersaturated N<sub>2</sub>O waters have been previously reported from the Baltic Sea: Rönner (1983)  
278 observed a N<sub>2</sub>O surface saturation of 79% in the central Baltic Sea and attributed the  
279 undersaturation to upwelling of N<sub>2</sub>O-depleted waters. Bange et al. (1998) found a minimum N<sub>2</sub>O  
280 saturation of 91% in the southern Baltic Sea where the hydrographic conditions were  
281 significantly influenced by riverine runoff. Walter et al. (2006) reported a mean N<sub>2</sub>O saturation  
282 of  $79\pm 11\%$  for shallow stations (<30 m) in the southwestern Baltic Sea in October 2003. The  
283 low-N<sub>2</sub>O event at BE was unusual because the concentrations were much lower than those  
284 reported values and it lasted for more than half a year.

285 Although the observed temperatures and salinities during October 2016–April 2017 were  
286 comparable to other years (Fig. S1), it is difficult to evaluate the role of physical mechanism in  
287 the low-N<sub>2</sub>O event because of insufficient data for water mass exchange at the BE Time-Series

288 Station. Here we mainly focused on the chemical or biological processes. Anoxia events with the  
289 presence of H<sub>2</sub>S were observed in the bottom waters for three months in a row during  
290 September–November 2016. This is an unusual long period and is unprecedented at the BE  
291 Time-Series Station. In December 2016 the stratification did not completely break down.  
292 Although the water column was generally oxygenated, bottom O<sub>2</sub> concentrations were the lowest  
293 observed during the past ten years. Considering the classical view of N<sub>2</sub>O consumption via  
294 denitrification under hypoxic and anoxic conditions, we inferred that denitrification accounted  
295 for low N<sub>2</sub>O concentrations in the bottom layer. However, the question still remains where the  
296 low-N<sub>2</sub>O-concentration water in the upper layers came from.

297 In September 2016, low N<sub>2</sub>O concentrations were only observed in the bottom waters where the  
298 anoxia occurred. However, the situation was different in the following months. During  
299 October/November 2016, N<sub>2</sub>O concentrations were homogeneously distributed in the water  
300 column. Although the stratification gradually started to break down in late autumn, the density  
301 gradient was still strong enough to keep the bottom waters at anoxic conditions and prevented  
302 the low-N<sub>2</sub>O-concentration to reach the surface. Thus we inferred that the unusual low N<sub>2</sub>O  
303 concentrations in the upper layers (above 20 m) were probably resulting from advection of  
304 adjacent waters. Due to the fact that the upper layers were well-mixed and oxygenated, in situ  
305 N<sub>2</sub>O consumption in the water column could be neglected. We suggest therefore, that the N<sub>2</sub>O  
306 depleted waters were resulting from consumption of N<sub>2</sub>O in bottom waters elsewhere and then  
307 they were upwelled and transported to BE. Hence, N<sub>2</sub>O consumption via denitrification might  
308 have been, directly or indirectly, responsible for the low N<sub>2</sub>O concentrations during October–  
309 November 2016.

310 In December 2016, the bottom waters were ventilated with O<sub>2</sub>. Although N<sub>2</sub>O consumption by  
311 denitrification should have been inhibited by the high concentrations of O<sub>2</sub> (Codispoti et al.,  
312 2001), the N<sub>2</sub>O concentrations did not restore to their normal level under suboxic conditions.  
313 Since January 2017, the whole water column was well mixed and oxygenated. Usually a  
314 significant nutrient supply could be observed starting in November (Fig. 4) as a result of  
315 remineralization and vertical mixing, but the average NO<sub>2</sub><sup>-</sup> and NO<sub>3</sub><sup>-</sup> concentrations during  
316 November 2016–April 2017 were 0.2 and 1.4 μM, respectively, which was about 50% and 60%  
317 lower than in other years. Ammonium (NH<sub>4</sub><sup>+</sup>) and chlorophyll *a* concentrations during this  
318 period were comparable to that of other years (Fig. S1). Secchi depth, a proxy of water  
319 transparency, was 3.8 m in March 2017, which is only slightly lower compared to the monthly  
320 average value for March (4.5±1.8 m). There is no exceptional spring algae bloom and thus we  
321 infer that assimilative uptake of nutrients by phytoplankton was not responsible for the low  
322 nutrients concentrations. The nutrient deficiency might be attributed to enhanced nitrogen  
323 removal processes like denitrification or anammox (Voss et al., 2005; Hietanen et al., 2007;  
324 Hannig et al., 2007) during the prolonged period of anoxia in autumn 2016. During the low N<sub>2</sub>O  
325 event, we found that N<sub>2</sub>O concentrations were positively correlated with both NO<sub>2</sub><sup>-</sup>  
326 ([N<sub>2</sub>O]=7.02[NO<sub>2</sub><sup>-</sup>]+7.36, R<sup>2</sup>=0.29, n=24, p<0.01) and NO<sub>3</sub><sup>-</sup> ([N<sub>2</sub>O]=0.80[NO<sub>3</sub><sup>-</sup>]+7.36, R<sup>2</sup>=0.51,

327 n=24,  $p < 0.0001$ ). These results indicate that the development and maintenance of the low-N<sub>2</sub>O-  
328 concentration was closely associated with nutrient deficiency. Especially after the breakdown of  
329 the stratification, when denitrification was no longer a significant N<sub>2</sub>O sink, nutrients might have  
330 become a limiting factor for N<sub>2</sub>O production.

331 In general, the low-N<sub>2</sub>O-concentration event during October 2016–April 2017 can be divided  
332 into two parts: in the stratified waters during October–November 2016, O<sub>2</sub> played a dominant  
333 role and N<sub>2</sub>O was consumed via denitrification under anoxic conditions. In the well-mixed water  
334 column during December 2016–April 2017, nutrient deficiency seemed to have constrained N<sub>2</sub>O  
335 production via nitrification under suboxic/oxic conditions.

336 In recent years a novel biological N<sub>2</sub>O consumption pathway, called N<sub>2</sub>O fixation, which  
337 transforms N<sub>2</sub>O into particulate organic nitrogen via its assimilation, has been reported (Farías et  
338 al., 2013). This process can take place under extreme environmental conditions even at very low  
339 N<sub>2</sub>O concentrations. Cornejo et al. (2015) reported that N<sub>2</sub>O fixation might play a major role in  
340 the coastal zone off central Chile where seasonally occurring surface N<sub>2</sub>O undersaturation was  
341 observed. The relatively high N<sub>2</sub> fixation rates in the Baltic Sea (Sohm et al., 2011) highlight the  
342 potential role of N<sub>2</sub>O fixation (Farías et al., 2013). However, we cannot quantify the role of  
343 biological N<sub>2</sub>O fixation for the N<sub>2</sub>O depletion in the Baltic Sea due to the absence of N<sub>2</sub>O  
344 assimilation measurements.

### 345 **3.4.2 High N<sub>2</sub>O concentrations in November 2017**

346 High N<sub>2</sub>O concentrations were observed at the BE Time-Series Station in November 2017. The  
347 average value reached  $35.4 \pm 1.5$  nM, which was the highest concentration measured during the  
348 entire sampling period from 2005 to 2017. Dissolved N<sub>2</sub>O was homogeneously distributed in the  
349 water column, but this event did not last long. In December, dissolved N<sub>2</sub>O returned to normal  
350 levels and the average concentration in the water column was comparable to that of other years.  
351 Average N<sub>2</sub>O saturation in November 2017 was  $322 \pm 10\%$ , which was also the highest for the  
352 past 12.5 years. This value was much higher than the maximum surface N<sub>2</sub>O saturation reported  
353 by Rönner (1983) in the central Baltic Sea, but was comparable to the results observed in the  
354 southern Baltic Sea (312%, Bange et al., 1998). Bange et al. (1998) linked the enhanced N<sub>2</sub>O  
355 concentrations to riverine runoff because those samples were collected in an estuarine area,  
356 however, the riverine influence around the BE Time-Series Station is negligible. As a result, the  
357 impact of fresh water input can be excluded.

358 Dissolved O<sub>2</sub> seemed to play a dominant role in the high N<sub>2</sub>O concentrations. Enhanced N<sub>2</sub>O  
359 production usually occurred at the oxic/anoxic interface, which was closely linked to the  
360 development of water column stratification. In general the breakdown of the stratification is  
361 faster than its establishment at the BE Time-Series Station. As a result, it took about half a year  
362 for bottom O<sub>2</sub> saturation to gradually decrease from ~80% to almost 0% (i.e. anoxia), but only  
363 two months to restore normal saturation level in 2010 (Fig. 6). In late autumn, surface water

364 penetrated into the deep layers via vertical mixing and eroded the oxic/anoxic interface. The  
365 entire water column quickly became oxygenated and the enhanced N<sub>2</sub>O production was stopped.

366 Hypoxia/anoxia at BE is usually observed in the bottom waters in autumn, but in September  
367 2017, hypoxic water (O<sub>2</sub> saturation < 20 %, which was close to the criterion for hypoxia, see  
368 Naqvi et al., 2010) was found in the subsurface layer (10 m) as well. Surface O<sub>2</sub> saturation was  
369 only ~50%, which was the lowest during the sampling period 2005–2017. The density gradient  
370 of the water column in September 2017 was much lower than in other years. These results  
371 indicate the occurrence of an upwelling event at BE Time-Series Station in autumn 2017, which  
372 might be a result of the saline water inflow from the North Sea considering the change of salinity  
373 in the water column (Fig. S1). Strong vertical mixing has interrupted the hypoxia/anoxia and  
374 bottom O<sub>2</sub> saturation reached ~60% in October 2017. The presence of O<sub>2</sub> prevented N<sub>2</sub>O  
375 consumption via denitrification, as a result, we did not observe a significant N<sub>2</sub>O decline during  
376 that period (Fig. 5).

377 Considering the fact that a significant autumn algae bloom was observed in autumn 2017 (as  
378 indicated by high chlorophyll a concentrations, see Fig. S1), severe O<sub>2</sub> depletion in the bottom  
379 water could be expected. Although the bottom O<sub>2</sub> saturation was only slightly lower in  
380 November than in October, we speculate that even lower O<sub>2</sub> saturation (but not anoxia) might  
381 have occurred between October and November. The “W-shaped” O<sub>2</sub> saturation curve (see Fig. 6)  
382 suggests that the stratification did not completely break down in October and that there might  
383 have been a reestablishment of the oxic/anoxic interface providing favorable conditions for  
384 enhanced N<sub>2</sub>O production. Due to the degradation of organic nitrogen, NH<sub>4</sub><sup>+</sup> is released from the  
385 sediment into bottom waters (Dale et al., 2011), especially in autumn when O<sub>2</sub> is low (Fig. S2).  
386 NH<sub>4</sub><sup>+</sup> concentrations in November 2017 were lower than in other years (Fig. S1), and NO<sub>2</sub><sup>-</sup>  
387 concentrations were higher (Fig. 5), indicating that nitrification occurred in bottom waters. To  
388 this end, we suggest that the reestablishment of the oxic/anoxic interface promoted ammonium  
389 oxidation (the first step of nitrification). In this case, N<sub>2</sub>O could have temporarily accumulated  
390 because its consumption via denitrification was blocked. Meanwhile, the relatively low density  
391 gradient (i.e. low stratification) allowed upward mixing of the excess N<sub>2</sub>O to the surface.  
392 However, we inferred that that this phenomenon would only last for a few days due to the rapid  
393 breakdown of stratification at the BE Time-Series Station.

394 Due to the development of the pronounced stratification, the oxic/anoxic interface prevailed in  
395 summer/early autumn as well, but we did not observe N<sub>2</sub>O accumulation during these months.  
396 One of the potential explanations is that enhanced N<sub>2</sub>O production only took place within  
397 particular depths where strong O<sub>2</sub> gradient existed, but our vertical sampling resolution was too  
398 low to capture this event. Also enhanced N<sub>2</sub>O production might be covered by the weak mixing  
399 which brought low-N<sub>2</sub>O water from the bottom to the surface.

400 The upwelling event played different roles in autumn 2016 and 2017. First, upwelling took place  
401 somewhere else but at BE because of the strong density and O<sub>2</sub> gradient in the water column

402 during autumn 2016. Second, bottom water remained anoxic in autumn 2016, while the  
403 compensated water for upwelling in 2017 penetrated through stratification and brought O<sub>2</sub> into  
404 bottom water (Fig. 6), which caused enhanced N<sub>2</sub>O production. Similarly, autumn upwelling was  
405 detected in 2011 and 2012 when we found relatively low O<sub>2</sub> concentrations in subsurface layers  
406 (10 m) (Fig. 2), but we did not observe an increase in bottom O<sub>2</sub> concentrations and N<sub>2</sub>O  
407 concentrations remained low during that time. These upwelling events seem to be driven by  
408 saline water inflow considering the prominent increase in salinity, but the mechanism dominates  
409 O<sub>2</sub> input into bottom water before the stratification break down remains unclear.

### 410 **3.5 Flux density**

411 During 2005–2017, surface N<sub>2</sub>O saturations at the BE Time-Series Station varied from 56 % to  
412 314 % (69–194 % excluding the extreme values discussed in Sect. 3.4), with an average of  
413 111±30 % (111±20 % without the extreme values). Generally the water column at BE was  
414 slightly oversaturated with N<sub>2</sub>O. Our results are in good agreement with the estimated mean  
415 surface N<sub>2</sub>O saturation for the European shelf (113%, Bange, 2006).

416 We found a weak seasonal cycle for surface N<sub>2</sub>O concentrations, with high N<sub>2</sub>O concentrations  
417 occurring in winter/early spring and low concentrations occurring in summer/autumn, but no  
418 such cycle for N<sub>2</sub>O saturation (Fig. 4; Fig. 7). The seasonality in concentration but not in  
419 saturation could be largely attributed to the effect of temperature on N<sub>2</sub>O solubility: In summer  
420 when surface N<sub>2</sub>O concentrations are low, N<sub>2</sub>O saturations are increased by the relative high  
421 temperature; and vice versa in winter. Although salinity also affects N<sub>2</sub>O solubility, its  
422 contribution is negligible compared to temperature. Temperature alleviated the fluctuation of  
423 surface N<sub>2</sub>O saturation and thus affected the sea-to-air N<sub>2</sub>O fluxes. We conclude that temperature  
424 plays a modulating role for N<sub>2</sub>O emissions.

425 The wind speed ( $u_{10}$ ) at the BE Time-Series Station ranged from 1.1 to 14.0 m s<sup>-1</sup>, with an  
426 average of 7.0±2.7 m s<sup>-1</sup>. N<sub>2</sub>O flux densities varied from -19.0 to 105.7 μmol m<sup>-2</sup> d<sup>-1</sup> (-14.1–30.3  
427 μmol m<sup>-2</sup> d<sup>-1</sup> without the extreme values), with an average of 3.5±12.4 μmol m<sup>-2</sup> d<sup>-1</sup> (3.3±6.5  
428 μmol m<sup>-2</sup> d<sup>-1</sup> without the extreme values). However, the true emissions might have been  
429 underestimated because our monthly sampling resolution is insufficient to capture short-term  
430 N<sub>2</sub>O accumulation events due to the fast breakdown of stratification in autumn. The uncertainty  
431 introduced in the flux density computation was estimated to be 20% (Wanninkhof, 2014). The  
432 flux densities at the BE Time-Series Station are comparable to those reported by Bange et al.  
433 (1998, 0.4–7.1 μmol m<sup>-2</sup> d<sup>-1</sup>) from the coastal waters of the southern Baltic Sea, but are slightly  
434 lower than the average N<sub>2</sub>O flux density reported by Rönner (1983, 8.9 μmol m<sup>-2</sup> d<sup>-1</sup>) from the  
435 central Baltic Sea. Please note that the results of Rönner (1983) were obtained only from the  
436 summer season and therefore are probably biased because of missing seasonality.

437 In December 2014, a strong saline water inflow from the North Sea was observed, which was the  
438 third strongest ever recorded (Mohrholz et al., 2015). Although the salinity in December 2014

439 was comparable to other years, a remarkable increase in salinity was observed in the following  
440 several months. However, we did not detect a significant N<sub>2</sub>O anomaly or enhanced emission  
441 during that time. Similarly, Walter et al. (2006) investigated the impact of the North Sea water  
442 inflow on N<sub>2</sub>O production in the southern and central Baltic Sea in 2003. The oxygenated water  
443 ventilated the deep Baltic Sea and shifted anoxic to oxic condition which led to enhanced N<sub>2</sub>O  
444 production, but the accumulated N<sub>2</sub>O was unlikely to reach the surface due to the presence of a  
445 permanent halocline (Walter et al., 2006).

446 Although we observed extremely high N<sub>2</sub>O flux density in November 2017, the low-N<sub>2</sub>O-  
447 concentration (<10 nM) events have become more and more frequent during the past ten years  
448 (Fig. 2). This phenomenon seldom occurred before 2011, but remarkable low N<sub>2</sub>O  
449 concentrations can be seen in 2011 and 2013, and to a less extent in 2012 and 2014. Similar  
450 events lasted for several months in 2015 and for even more than half a year during 2016–2017.  
451 The most striking was that the low-N<sub>2</sub>O-concentration water was not only detected in bottom  
452 waters, but also at surface which would significantly impact the air-sea N<sub>2</sub>O flux densities.  
453 Although the MKT result did not give a significant trend for the N<sub>2</sub>O flux densities, the data  
454 presented in Fig. 8 suggest a potential decline of N<sub>2</sub>O flux densities from the coastal Baltic Sea,  
455 challenging the conventional view that N<sub>2</sub>O emissions from coastal waters would most probably  
456 increase in the future, which was based on the hypothesis of increasing nutrient loads into coastal  
457 waters. Due to an effective reduction of nutrient inputs, the severe eutrophication condition in the  
458 Baltic Sea has been alleviated (HELCOM, 2018b), but ongoing deoxygenation points to the fact  
459 that it will take a longer time for coastal ecosystems to feedback to reduced nutrient inputs  
460 because other environmental changes such as warming may override decreasing eutrophication  
461 (Lennartz et al., 2014).

## 462 **4. Conclusions**

463 The seasonal and inter-annual N<sub>2</sub>O variations at the BE Time-Series Station from July 2005 to  
464 December 2017 were driven by the prevailing O<sub>2</sub> regime and nutrients availability. We found a  
465 pronounced seasonal cycle with low N<sub>2</sub>O concentrations (undersaturations) occurring in  
466 hypoxic/anoxic bottom waters in autumn and enhanced concentrations (supersaturations) all over  
467 the water column in winter/early spring. Significant decreasing trends for N<sub>2</sub>O concentrations  
468 were found for few months, while most of the year, no significant trend was detectable in the  
469 period of 2005–2017. During 2005–2017, no significant trends were present for O<sub>2</sub> and nutrients  
470 either, but these parameters all show significant decreasing trends on longer time scales (~60  
471 years) at BE. Our results show the strong coupling of N<sub>2</sub>O with O<sub>2</sub> and nutrient concentrations,  
472 and suggest similar changes on comparable time scales. Further monitoring of N<sub>2</sub>O at BE time  
473 series station is thus important to detect changes. Further studies on N<sub>2</sub>O  
474 production/consumption by nitrification and denitrification and analysis of the characteristic N<sub>2</sub>O  
475 isotope signature might be very helpful to decipher the potential roles of O<sub>2</sub>/nutrients for N<sub>2</sub>O  
476 cycling.

477 Temperature plays a modulating role for the N<sub>2</sub>O emission at the BE Time-Series Station.  
478 Although the hydrographic condition at BE is generally dominated by the inflow of saline North  
479 Sea water, this did not affect N<sub>2</sub>O production and its emissions to the atmosphere. It seems that  
480 events with extremely low N<sub>2</sub>O concentrations and thus reduced N<sub>2</sub>O emissions became more  
481 frequent in recent years. Our results provide a new perspective onto potential future patterns of  
482 N<sub>2</sub>O distribution and emissions in coastal areas. Continuous measurement at the BE Time-Series  
483 Station with a focus on late autumn would be of great importance for monitoring and  
484 understanding the future changes of N<sub>2</sub>O concentrations and emissions in the southwestern Baltic  
485 Sea.

## 486 **Data availability**

487 Data are available from the Boknis Eck Database: [www.bokniseck.de](http://www.bokniseck.de)

## 488 **Author contribution**

489 X.M., S.T.L. and H.W.B. designed the study and participated in the fieldwork. N<sub>2</sub>O  
490 measurements and data processing were done by X.M. and S.T.L. X.M. wrote the manuscript  
491 with contributions from S.T.L. and H.W.B.

## 492 **Competing interests**

493 The authors declare that they have no conflict of interest.

## 494 **Acknowledgments**

495 The authors thank the captain and crew of the RV *Littorina* and *Polarfuchs* as well as the many  
496 colleagues and numerous students who helped with the sampling and measurements of the BE  
497 time-series through various projects. Special thanks to A. Kock for her help with sampling,  
498 measurements and data analysis. The time-series at BE was supported by DWK  
499 Meeresforschung (1957–1975), HELCOM (1979–1995), BMBF (1995–1999), the Institut für  
500 Meereskunde (1999–2003), IfM-GEOMAR (2004–2011) and GEOMAR (2012–present). The  
501 current N<sub>2</sub>O measurements at BE are supported by the EU BONUS INTEGRAL project which  
502 receives funding from BONUS (Art 185), funded jointly by the EU, the German Federal  
503 Ministry of Education and Research, the Swedish Research Council Formas, the Academy of  
504 Finland, the Polish National Centre for Research and Development, and the Estonian Research  
505 Council. The Boknis Eck Time-Series Station ([www.bokniseck.de](http://www.bokniseck.de)) is run by the Chemical  
506 Oceanography Research Unit of GEOMAR, Helmholtz Centre for Ocean Research Kiel. Data  
507 from BE are available from [www.bokniseck.de/database-access](http://www.bokniseck.de/database-access). The N<sub>2</sub>O data presented here  
508 have been archived in MEMENTO (the MarinE MethanE and NiTrous Oxide database:  
509 <https://memento.geomar.de>). X. Ma is grateful to the China Scholarship Council for providing  
510 financial support (File No. 201306330056) and the EU BONUS INTEGRAL project.



## 511 **References**

- 512 Bange, H. W.: Nitrous oxide and methane in European coastal waters, *Estuar. Coast. Shelf S.*, 70,  
513 361–374, <https://doi.org/10.1016/j.ecss.2006.05.042>, 2006.
- 514 Bange, H. W., Dahlke, S., Ramesh, R., Meyer-Reil, L. A., Rapsomanikis, S., and Andreae, M. O.:  
515 Seasonal study of methane and nitrous oxide in the coastal waters of the southern Baltic Sea,  
516 *Estuar. Coast. Shelf S.*, 47, 807–817, <https://doi.org/10.1006/ecss.1998.0397>, 1998.
- 517 Battaglia, G. and Joos, F.: Marine N<sub>2</sub>O emissions from nitrification and denitrification  
518 constrained by modern observations and projected in multimillennial global warming simulations,  
519 *Global Biogeochem. Cy.*, 32, 92–121, <https://doi.org/10.1002/2017GB005671>, 2018.
- 520 Bonin, P., Gilewicz, M., and Bertrand, J. C.: Effects of oxygen on each step of denitrification on  
521 *Pseudomonas nautica*, *Can. J. Microbiol.*, 35, 1061–1064, <https://doi.org/10.1139/m89-177>, 1989.
- 522 Breitburg, D., Levin, L. A., Oschlies, A., Grégoire, M., Chavez, F. P., Conley, D. J., Garçon, V.,  
523 Gilbert, D., Gutiérrez, D., Isensee, K., Jacinto, G. S., Limburg, K. E., Montes, I., Naqvi, S. W. A.,  
524 Pitcher, G. C., Rabalais, N. N., Roman, M. R., Rose, K. A., Seibel, B. A., Telszewski, M.,  
525 Yasuhara, M., and Zhang, J.: Declining oxygen in the global ocean and coastal waters, *Science*,  
526 359, eaam7240, <http://dx.doi.org/10.1126/science.aam7240>, 2018.
- 527 Capelle, D. W., Hawley, A. K., Hallam, S. J., and Tortell, P. D.: A multi-year time-series of N<sub>2</sub>O  
528 dynamics in a seasonally anoxic fjord: Saanich Inlet, British Columbia, *Limnol. Oceanogr.*, 63,  
529 524–539, <https://doi.org/10.1002/lno.10645>, 2018.
- 530 Carstensen, J., Andersen, J. H., Gustafsson, B. G., and Conley, D. J.: Deoxygenation of the  
531 Baltic Sea during the last century, *P. Natl. Acad. Sci. USA*, 111, 5628–5633,  
532 <https://doi.org/10.1073/pnas.1323156111>, 2014.
- 533 Codispoti, L. A., Elkins, J. W., Yoshinari, T., Fredrich, G., Sakamoto, C., and Packard, T.: On  
534 the nitrous oxide flux from productive regions that contain low oxygen waters, in: *Oceanography*  
535 *of the Indian Ocean*, edited by Desai, B. N., Oxford Univ. Press, New York, 271–284, 1992.
- 536 Codispoti, L. A., Brandes, J. A., Christensen, J. P., Devol, A. H., Naqvi, S. W. A., Paerl, H. W.,  
537 and Yoshinari, T.: The oceanic fixed nitrogen and nitrous oxide budgets: Moving targets as we  
538 enter the anthropocene? *Sci. Mar.*, 65, 85–105, <https://doi.org/10.3989/scimar.2001.65s285>, 2001.
- 539 Codispoti, L. A., Yoshinari, T., and Devol, A. H.: Suboxic respiration in the oceanic water  
540 column, in: *Respiration in aquatic ecosystems*, edited by del Giorgio, P. A. and Williams, P. J.,  
541 Oxford Univ. Press, New York, 225–247, 2005.

542 Conley, D. J., Carstensen, J., Aigars, J., Axe, P., Bonsdorff, E., Eremina, T., and Lannegren, C.:  
543 Hypoxia is increasing in the coastal zone of the Baltic Sea, *Environ. Sci. Technol.*, 45, 6777–  
544 6783, doi: 10.1021/es201212r, 2011.

545 Cornejo, M., Murillo, A. A., and Farías, L.: An unaccounted for N<sub>2</sub>O sink in the surface water of  
546 the eastern subtropical South Pacific: Physical versus biological mechanisms, *Prog. Oceanogr.*,  
547 137, 12–23, <https://doi.org/10.1016/j.pocean.2014.12.016>, 2015.

548 Dale, A. W., Sommer, S., Bohlen, L., Treude, T., Bertics, V. J., Bange, H. W., Pfannkuche, O.,  
549 Schorp, T., Mattsdotter, M., and Wallmann, K.: Rates and regulation of nitrogen cycling in  
550 seasonally hypoxic sediments during winter (Boknis Eck, SW Baltic Sea): Sensitivity to  
551 environmental variables, *Estuar. Coast. Shelf S.*, 95, 14–28,  
552 <https://doi.org/10.1016/j.ecss.2011.05.016>, 2011.

553 Ducklow, H. W., Doney, S. C., and Steinberg, D. K.: Contributions of long-term research and  
554 time-series observations to marine ecology and biogeochemistry, *Annu. Rev. Mar. Sci.*, 1, 279–  
555 302, <https://doi.org/10.1146/annurev.marine.010908.163801>, 2009.

556 Farías, L., Castro-González, M., Cornejo, M., Charpentier, J., Faúndez, J., Boontanon, N., and  
557 Yoshida, N.: Denitrification and nitrous oxide cycling within the upper oxycline of the eastern  
558 tropical South Pacific oxygen minimum zone, *Limnol. Oceanogr.*, 54, 132–144,  
559 <https://doi.org/10.4319/lo.2009.54.1.0132>, 2009.

560 Farías, L., Faúndez, J., Fernández, C., Cornejo, M., Sanhueza, S., and Carrasco, C.: Biological  
561 N<sub>2</sub>O fixation in the Eastern South Pacific Ocean and marine cyanobacterial cultures, *Plos one*, 8,  
562 e63956, <https://doi.org/10.1371/journal.pone.0063956>, 2013.

563 Farías, L., Besoain, V., and García-Loyola, S.: Presence of nitrous oxide hotspots in the coastal  
564 upwelling area off central Chile: an analysis of temporal variability based on ten years of a  
565 biogeochemical time series, *Environ. Res. Lett.*, 10, 044017, doi:10.1088/1748-  
566 9326/10/4/044017, 2015.

567 Goreau, T. J., Kaplan, W. A., Wofsy, S. C., McElroy, M. B., Valois, F. W., and Watson, S.W.:  
568 Production of NO<sub>2</sub><sup>-</sup> and N<sub>2</sub>O by nitrifying bacteria at reduced concentrations of oxygen, *Appl.*  
569 *Environ. Microb.*, 40, 526–532, 1980.

570 Grasshoff, K., Kremling, K., and Ehrhardt, M.: *Methods of seawater analysis*, 3rd edition,  
571 WILEY-VCH, Weinheim, Germany, 1999.

572 Hannig, M., Lavik, G., Kuypers, M. M. M., Woebken, D., Martens-Habbena, W., and Jürgens,  
573 K.: Shift from denitrification to anammox after inflow events in the central Baltic Sea, *Limnol.*  
574 *Oceanogr.*, 52, 1336–1345, 2007.

575 Hansen, H. P., Giesenhausen, H. C., and Behrends, G.: Seasonal and long-term control of bottom  
576 water oxygen deficiency in a stratified shallow-coastal system, *ICES J. Mar. Sci.*, 56, 65–71, doi:  
577 10.1006/jmsc.1999.0629, 1999.

578 HELCOM: Sources and pathways of nutrients to the Baltic Sea, *Baltic Sea Environ. Proc.*, 153,  
579 2018a.

580 HELCOM: State of the Baltic Sea - Second HELCOM holistic assessment 2011–2016, *Baltic*  
581 *Sea Environ. Proc.*, 155, <http://stateofthebalticsea.helcom.fi/>, 2018b.

582 Hietanen, S., and Lukkari, K.: Effects of short-term anoxia on benthic denitrification, nutrient  
583 fluxes and phosphorus forms in coastal Baltic sediment, *Aquat. Microb. Ecol.*, 49, 293–302,  
584 <https://doi.org/10.3354/ame01146>, 2007.

585 Hsu, S. A., Meindl, E. A., and Gilhousen, D. B.: Determining the power-law wind-profile  
586 exponent under near-neutral stability conditions at sea, *J. Appl. Meteorol.*, 33, 757–765,  
587 [https://doi.org/10.1175/1520-0450\(1994\)033<0757:DTPLWP>2.0.CO;2](https://doi.org/10.1175/1520-0450(1994)033<0757:DTPLWP>2.0.CO;2), 1994.

588 IPCC: Climate Change 2013: The physical science basis. Contribution of Working Group I to the  
589 fifth assessment report of the Intergovernmental Panel on Climate Change, Cambridge  
590 University Press, Cambridge, UK and New York, NY, 2013.

591 Landolfi, A., Somes, C. J., Koeve, W., Zamora, L. M., and Oschlies, A.: Oceanic nitrogen  
592 cycling and N<sub>2</sub>O flux perturbations in the Anthropocene, *Global Biogeochem. Cy.*, 31, 1236–  
593 1255, doi:10.1002/2017GB005633, 2017.

594 Lennartz, S. T., Lehmann, A., Herrford, J., Malien, F., Hansen, H. P., Biester, H., and Bange, H.  
595 W.: Long-term trends at the Boknis Eck time series station (Baltic Sea), 1957–2013: does  
596 climate change counteract the decline in eutrophication? *Biogeosciences*, 11, 6323–6339,  
597 <https://doi.org/10.5194/bg-11-6323-2014>, 2014.

598 Löscher, C. R., Kock, A., Könneke, M., LaRoche, J., Bange, H. W., and Schmitz, R. A.:  
599 Production of oceanic nitrous oxide by ammonia-oxidizing archaea, *Biogeosciences*. 9, 2419–  
600 2429, <https://doi.org/10.5194/bg-9-2419-2012>, 2012.

601 Kock, A., Arévalo-Martínez, D. L., Löscher, C. R., and Bange, H. W.: Extreme N<sub>2</sub>O  
602 accumulation in the coastal oxygen minimum zone off Peru, *Biogeosciences*. 13, 827–840, doi:  
603 10.5194/bg-13-827-2016, 2016.

604 Kroeze, C., and Seitzinger, S. P.: Nitrogen inputs to rivers, estuaries and continental shelves and  
605 related nitrous oxide emissions in 1990 and 2050: a global model, *Nutr. Cycl. Agroecosys.*, 52,  
606 195–212, 1998.

607 Kulkarni, A., and Von Storch, H.: Monte Carlo experiments on the effect of serial correlation on  
608 the Mann-Kendall test of trend, *Meteorol. Z.*, 4, 82–85, 1995.

609 Martinez-Rey, J., Bopp, L., Gehlen, M., Tagliabue, A., and Gruber, N.: Projections of oceanic  
610 N<sub>2</sub>O emissions in the 21<sup>st</sup> century using the IPSL Earth system model, *Biogeosciences*, 12,  
611 4133–4148, doi: 10.5194/bg-12-4133-2015, 2015.

612 Meier, H. M., Väli, G., Naumann, M., Eilola, K., and Frauen, C.: Recently accelerated oxygen  
613 consumption rates amplify deoxygenation in the Baltic Sea, *J. Geophys. Res.-Oceans.*, 123,  
614 3227–3240, <https://doi.org/10.1029/2017JC013686>, 2018.

615 Mohrholz, V., Naumann, M., Nausch, G., Krüger, S., and Gräwe, U.: Fresh oxygen for the Baltic  
616 Sea-An exceptional saline inflow after a decade of stagnation, *J. Marine Syst.*, 148, 152-166,  
617 <https://doi.org/10.1016/j.jmarsys.2015.03.005>, 2015.

618 Naqvi, S. W. A., Jayakumar, D. A., Narvekar, P. V., Naik, H., Sarma, V. V. S. S., D'souza, W.,  
619 Joseph, S., and George, M. D.: Increased marine production of N<sub>2</sub>O due to intensifying anoxia  
620 on the Indian continental shelf, *Nature*, 408, 346, 2000.

621 Naqvi, S.W.A., Bange, H.W., Farías, L., Monteiro, P.M.S., Scranton, M.I., and Zhang, J.: Marine  
622 hypoxia/anoxia as a source of CH<sub>4</sub> and N<sub>2</sub>O, *Biogeosciences*, 7, 2159–2190,  
623 <https://doi.org/10.5194/bg-7-2159-2010>, 2010.

624 Nevison, C., Butler, J. H., and Elkins, J. W.: Global distribution of N<sub>2</sub>O and the ΔN<sub>2</sub>O-AOU  
625 yield in the subsurface ocean, *Global Biogeochem. Cy.*, 17,  
626 <https://doi.org/10.1029/2003GB002068>, 2003.

627 Nightingale, P., G. Malin, C. S. Law, A. J. Watson, P. S. Liss, M. I. Liddicoat, J. Boutin, and R.  
628 C. Upstill-Goddard: In situ evaluation of air-sea gas exchange parameterizations using novel  
629 conservative and volatile tracers, *Global Biogeochem. Cy.*, 14, 373–387,  
630 <https://doi.org/10.1029/1999GB900091>, 2000.

631 Rabalais, N. N., Cai, W.-J., Carstensen, J., Conley, D. J., Fry, B., Hu, X., Quinones-Rivera, Z.,  
632 Rosenberg, R., Slomp, C. P., Turner, R. E., Voss, M., Wissel, B., and Zhang, J.: Eutrophication-  
633 driven deoxygenation in the coastal ocean, *Oceanography*, 27, 172–183,  
634 <https://doi.org/10.5670/oceanog.2014.21>, 2014.

635 Ravishankara, A. R., Danielm J., S., and Portmann, R. W.: Nitrous oxide (N<sub>2</sub>O): the dominant  
636 ozone-depleting substance emitted in the 21<sup>st</sup> century, *Science*, 326, 123–125, doi:  
637 10.1126/science.1176985, 2009.

638 Rönner, U.: Distribution, production and consumption of nitrous oxide in the Baltic Sea,  
639 *Geochim. Cosmochim. Ac.*, 47, 2179–2188, [https://doi.org/10.1016/0016-7037\(83\)90041-8](https://doi.org/10.1016/0016-7037(83)90041-8),  
640 1983.

641 Schlittgen, R., and Streitberg, B. H. J.: *Zeitreihenanalyse*, Oldenburg Wissenschaftsverlag,  
642 Munich, Germany, 2001.

643 Seitzinger, S. P., and Kroeze, C.: Global distribution of nitrous oxide production and N inputs in  
644 freshwater and coastal marine ecosystems, *Global Biogeochem. Cy.*, 12, 93–113, 1998.

645 Siedler, G., and Peters, H.: Properties of sea water, in: *Oceanography*, edited by Sündermann J.,  
646 Springer, Berlin, Heidelberg, 233–264, 1986.

647 Simone, F.: Mann-Kendall Test, MathWorks,  
648 <https://ww2.mathworks.cn/matlabcentral/fileexchange/25531-mann-kendall-test>, 2009.

649 Sohm, J. A., Webb, E. A., and Capone, D. G.: Emerging patterns of marine nitrogen fixation, *Nat.*  
650 *Rev. Microbiol.*, 9, 499–508, doi: 10.1038/nrmicro2594, 2011.

651 Tiedje, J. M.: Ecology of denitrification and dissimilatory nitrate reduction to ammonium, in:  
652 *Environmental Microbiology of Anaerobes*, edited by: Zehnder, A. J. B., John Wiley & Sons,  
653 N.Y., 179–244, 1988.

654 Torrence, C., and Compo, G. P.: A practical guide to wavelet analysis, *B. Am. Meteorol. Soc.*,  
655 79, 61–78, [https://doi.org/10.1175/1520-0477\(1998\)079<0061:APGTWA>2.0.CO;2](https://doi.org/10.1175/1520-0477(1998)079<0061:APGTWA>2.0.CO;2), 1998.

656 Torrence, C., and Compo, G. P.: Wavelet analysis, <http://paos.colorado.edu/research/wavelets/>,  
657 2004.

658 Voss, M., Emeis, K. C., Hille, S., Neumann, T., and Dippner, J. W.: Nitrogen cycle of the Baltic  
659 Sea from an isotopic perspective, *Global Biogeochem. Cy.*, 19, doi: 10.1029/2004GB002338,  
660 2005.

661 Walter, S., Breitenbach, U., Bange, H. W., Nausch, G., and Wallace, D. W.: Distribution of N<sub>2</sub>O  
662 in the Baltic Sea during transition from anoxic to oxic conditions, *Biogeosciences*, 3, 557–570,  
663 <https://doi.org/10.5194/bg-3-557-2006>, 2006.

664 Wanninkhof, R.: Relationship between wind speed and gas exchange over the ocean revisited,  
665 *Limnol. Oceanogr.: Methods*, 12, 351–362, <https://doi.org/10.4319/lom.2014.12.351>, 2014.

666 Weiss, R. F., and Price, B. A.: Nitrous oxide solubility in water and seawater, *Mar. Chem.*, 8,  
667 347–359, [https://doi.org/10.1016/0304-4203\(80\)90024-9](https://doi.org/10.1016/0304-4203(80)90024-9), 1980.

668 Wilson, S. T., Ferrón, S., and Karl, D. M.: Interannual variability of methane and nitrous oxide in  
669 the North Pacific Subtropical Gyre, *Geophys. Res. Lett.*, 44, 9885–9892,  
670 <https://doi.org/10.1002/2017GL074458>, 2017.

671 Xu, Z. X., Takeuchi, K., and Ishidaira, H.: Monotonic trend and step changes in Japanese  
672 precipitation, *J. Hydrol.*, 279, 144–150, [https://doi.org/10.1016/S0022-1694\(03\)00178-1](https://doi.org/10.1016/S0022-1694(03)00178-1), 2003.

673 Yang, D., Li, C., Hu, H., Lei, Z., Yang, S., Kusuda, T., Koike, T., and Musiaka, K.: Analysis of  
674 water resources variability in the Yellow river of China during the last half century using the  
675 historical data, *Water Resour. Res.*, 40, 1–12, <https://doi.org/10.1029/2003WR002763>, 2004.

676 Zhang, G.-L., Zhang, J., Liu, S.-M., Ren, J.-L., and Zhao, Y.-C.: Nitrous oxide in the Changjiang  
677 (Yangtze River) estuary and its adjacent marine area: Riverine input, sediment release and  
678 atmospheric fluxes, *Biogeosciences*, 7, 3505–3516, <https://doi.org/10.5194/bg-7-3505-2010>,  
679 2010.

680 Table 1. The results of the Mann-Kendall test for the surface and bottom N<sub>2</sub>O concentrations and  
 681 saturations of the 12 individual months.

682 Table 1a. MKT results for N<sub>2</sub>O concentrations

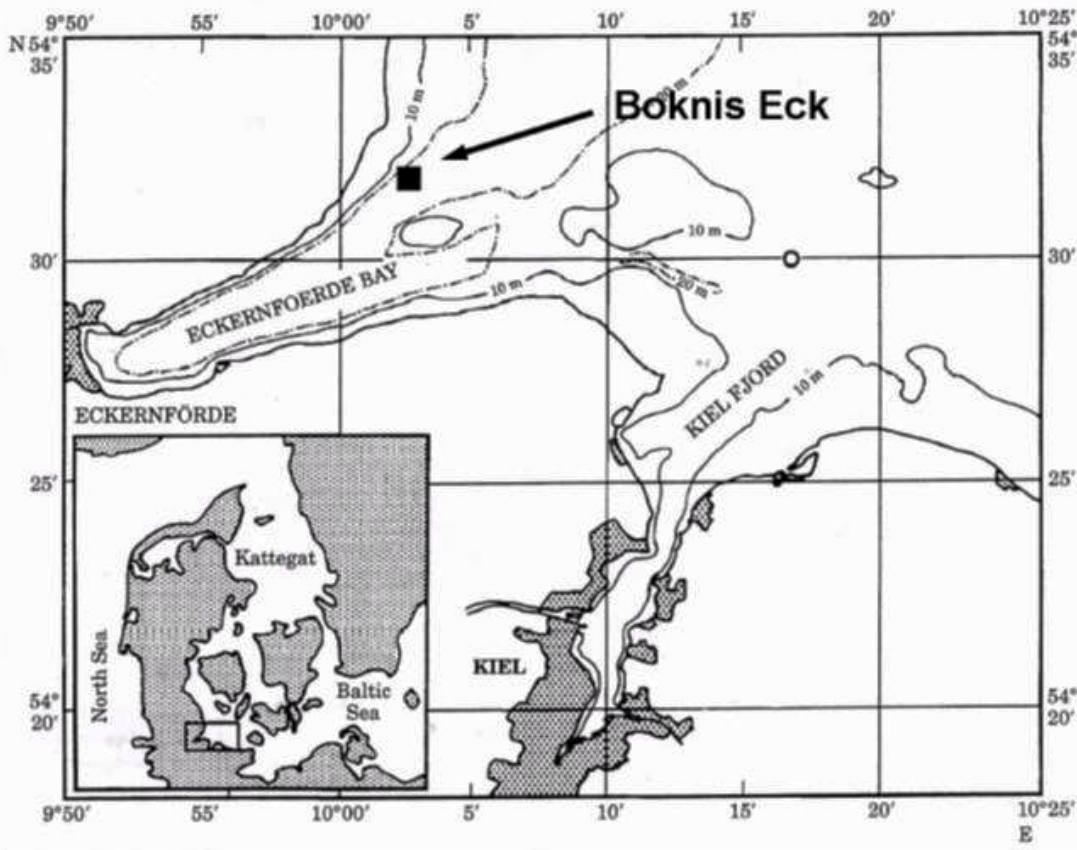
Month	January		February		March		April	
Depth/m	1	25	1	25	1	25	1	25
p	0.09	0.19	0.11	0.03(-)	0.19	0.63	0.09	0.30
Month	May		June		July		August	
Depth/m	1	25	1	25	1	25	1	25
p	0.63	0.24	0.15	0.95	0.16	0.16	0.20	0.03(-)
Month	September		October		November		December	
Depth/m	1	25	1	25	1	25	1	25
p	0.25	0.76	0.36	0.76	0.67	0.16	0.10	0.30

683

684 Table 1b. MKT results for N<sub>2</sub>O saturations

Month	January		February		March		April	
Depth/m	1	25	1	25	1	25	1	25
p	0.37	0.24	0.15	0.15	0.19	0.63	0.11	0.19
Month	May		June		July		August	
Depth/m	1	25	1	25	1	25	1	25
p	0.19	1	0.37	0.54	0.10	0.43	0.20	0.02(-)
Month	September		October		November		December	
Depth/m	1	25	1	25	1	25	1	25
p	0.04(-)	0.85	0.06	0.43	0.20	0.03(-)	0.16	0.36

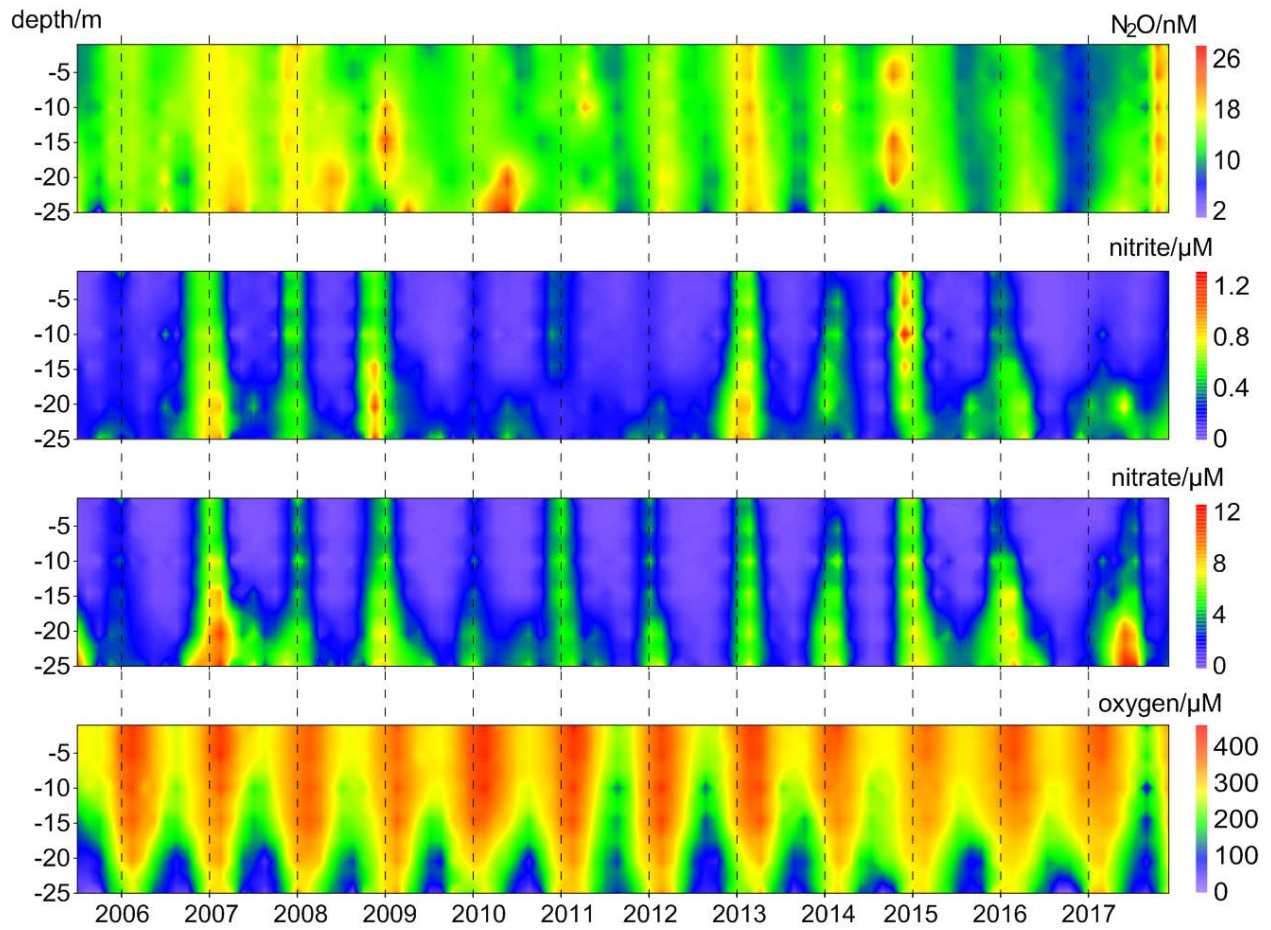
685  
 686 p indicates the p-value of the test, which is the probability, under the null hypothesis, of obtaining a value of  
 687 the test statistic as extreme or more extreme than the value computed from the sample.  
 688 (-) indicates a rejection of the null hypothesis at  $\alpha$  significance level and a decreasing trend is detected.



689

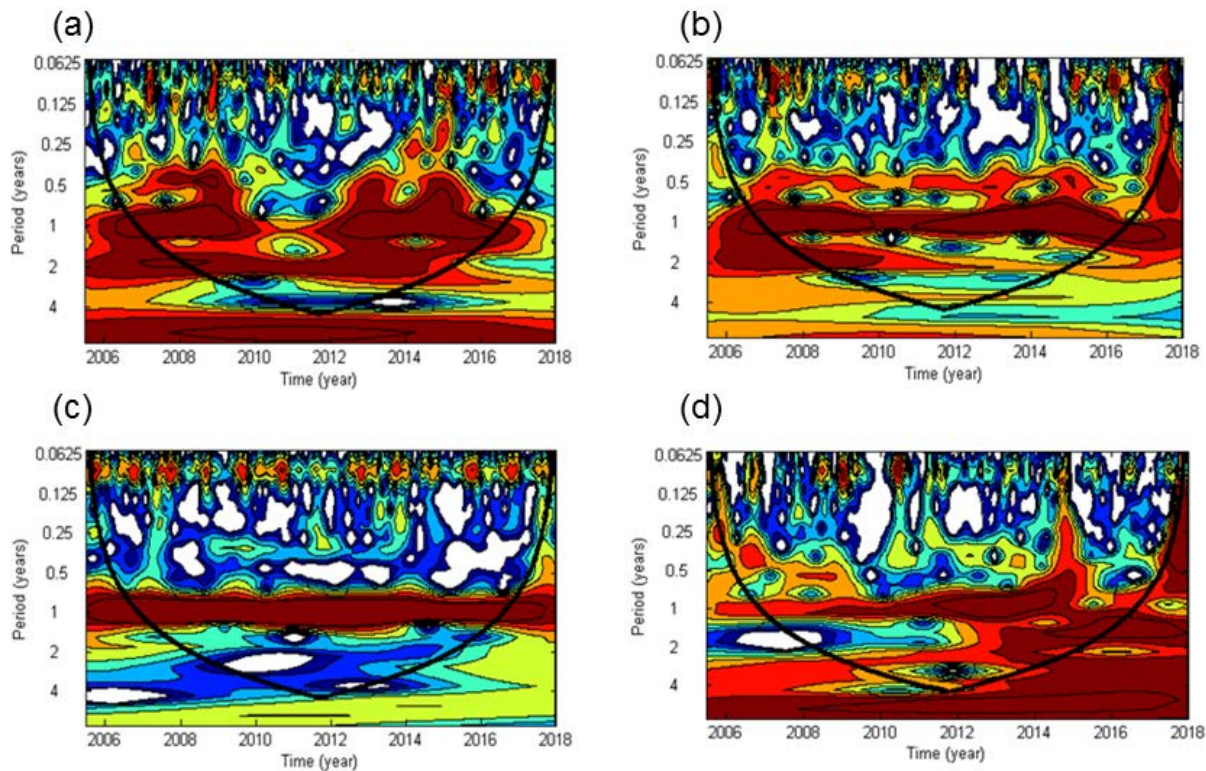
690 Fig. 1 Location of the Boknis Eck Time-Series Station in the Eckernförde Bay, southwestern Baltic Sea. (Map  
 691 from Hansen et al., 1999)





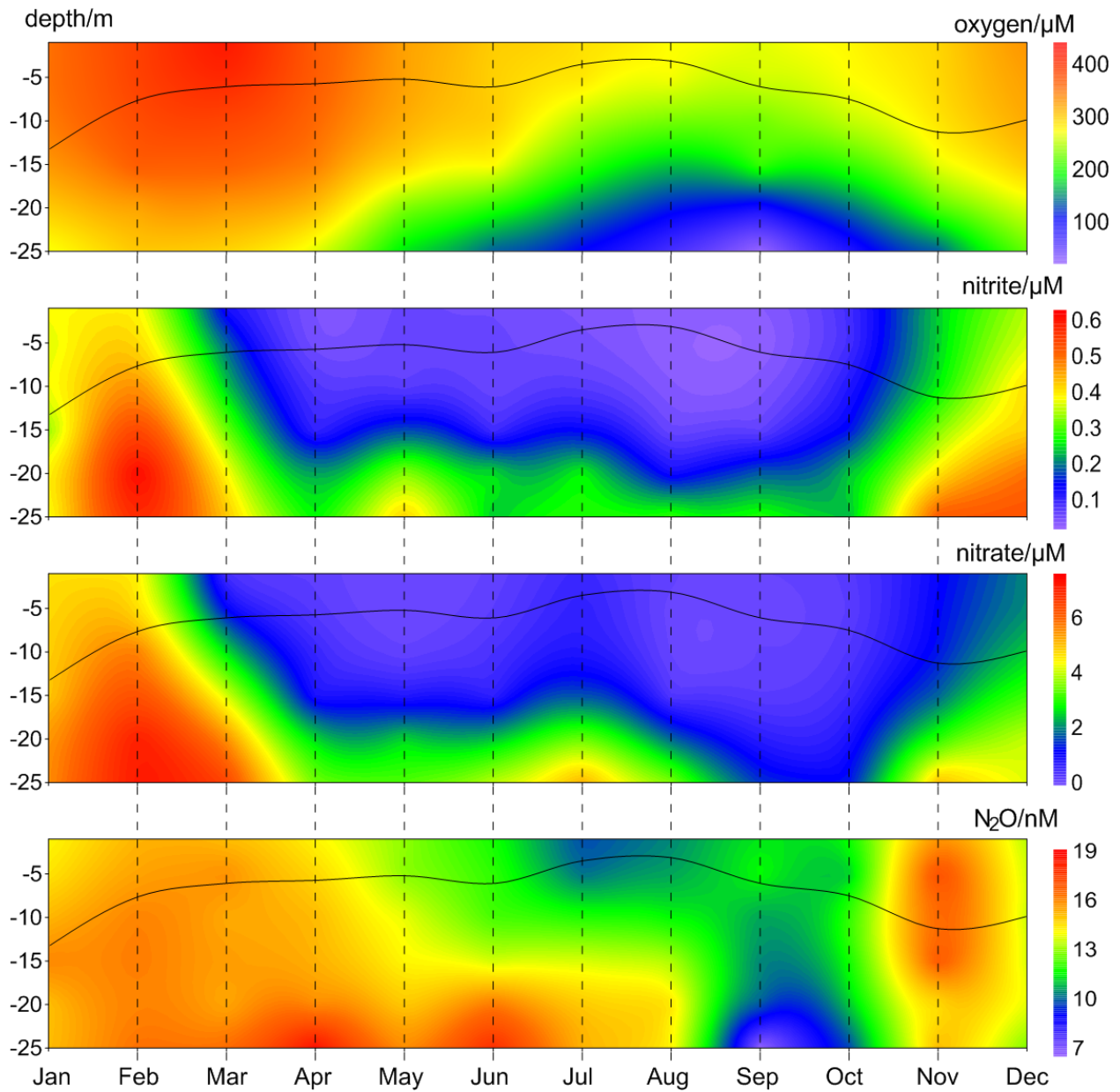
692

693 Fig. 2 Vertical distributions of dissolved O<sub>2</sub>, NO<sub>2</sub><sup>-</sup>, NO<sub>3</sub><sup>-</sup>, and N<sub>2</sub>O from the BE Time-Series Station during  
 694 2005–2017.



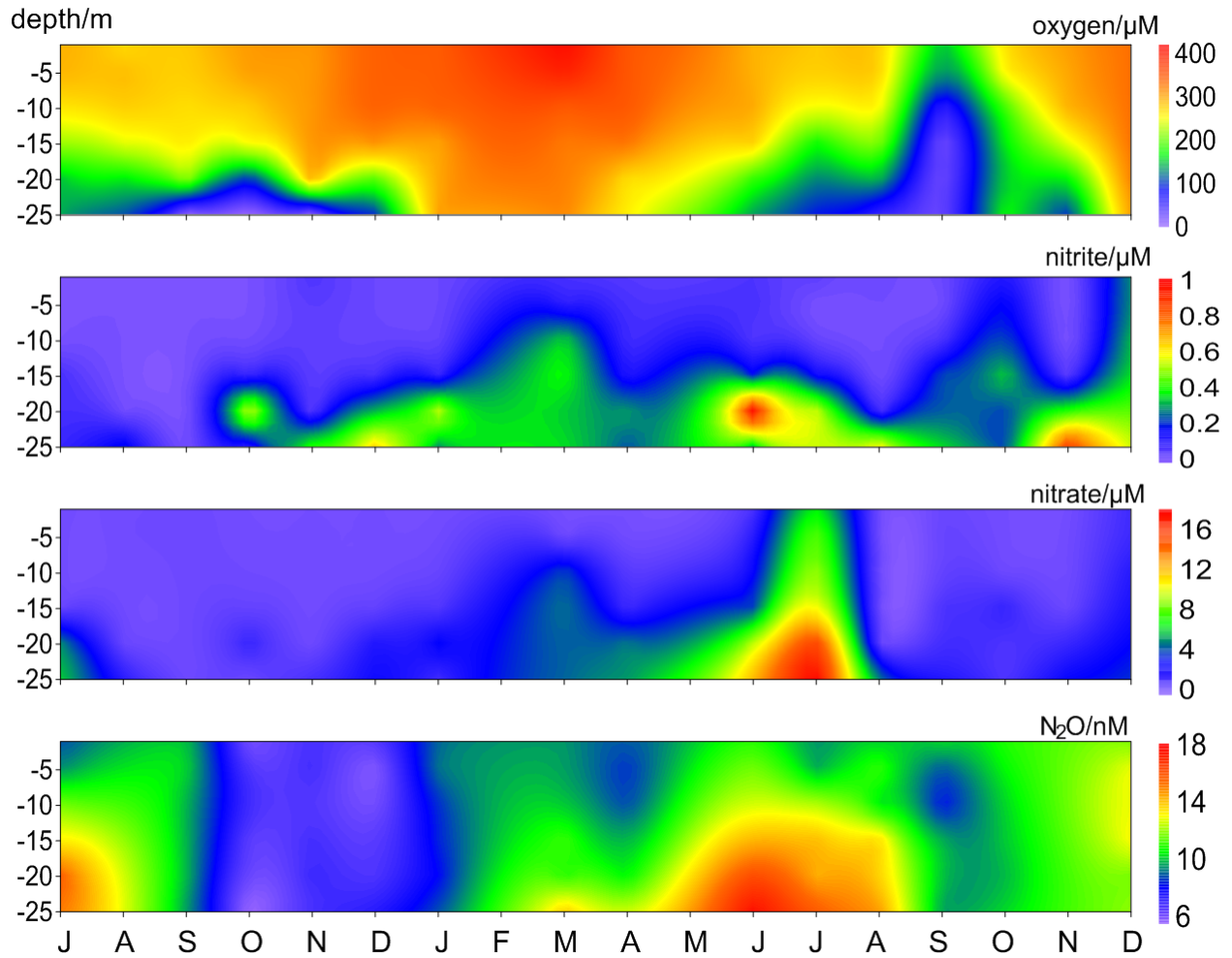
695

696 Fig. 3 Wavelet power spectra of  $\text{NO}_2^-$  (a),  $\text{NO}_3^-$  (b), dissolved  $\text{O}_2$  (c) and  $\text{N}_2\text{O}$  (d) from the BE Time-Series  
 697 Station. Red areas indicate high, blue indicate low power. The black conic line indicates the significant area  
 698 where boundary effects can be excluded.

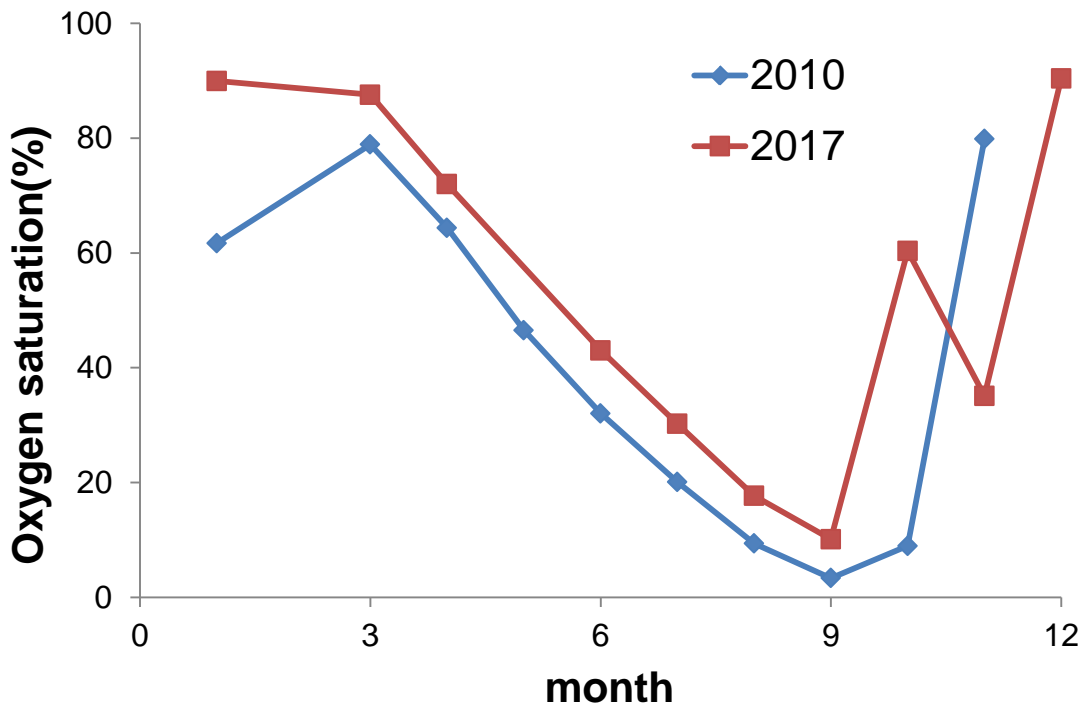


699

700 Fig. 4 Average vertical distributions of dissolved  $O_2$ ,  $NO_2^-$ ,  $NO_3^-$ , and  $N_2O$  from the BE Time-Series Station  
 701 during 2005–2017. The black line indicates the mixed layer depth, which was calculated based on a potential  
 702 density anomaly of  $0.15 \text{ kg m}^{-3}$  from the sea surface (1m).

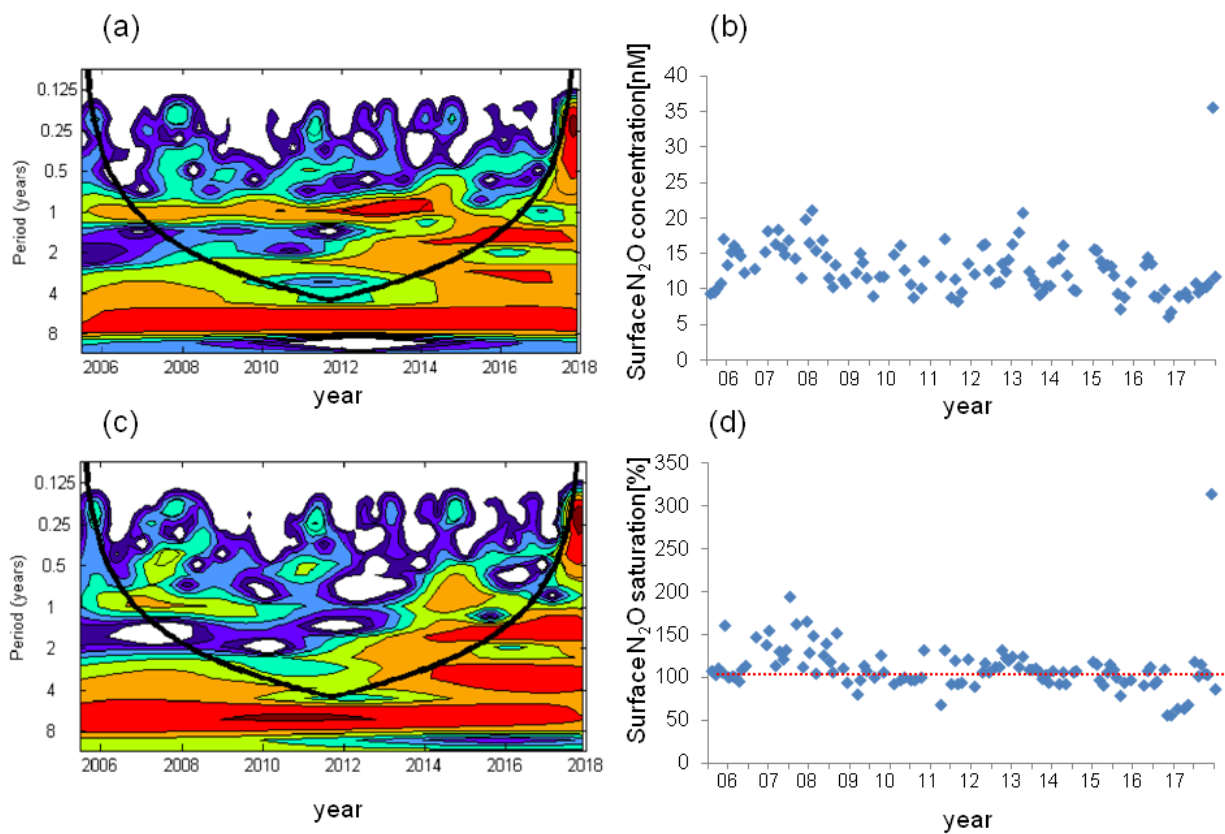


703  
 704 Fig. 5 Vertical distribution of dissolved O<sub>2</sub>, NO<sub>2</sub><sup>-</sup>, NO<sub>3</sub><sup>-</sup>, and N<sub>2</sub>O from the BE Time-Series Station during July  
 705 2016–December 2017. Please note that the high N<sub>2</sub>O concentrations in November 2017 were removed for  
 706 better visualization.



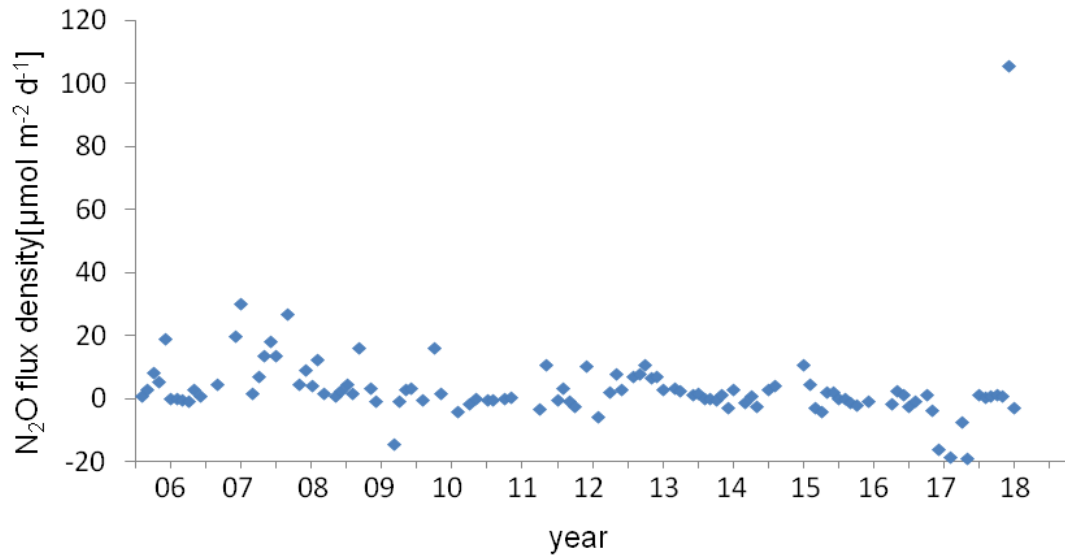
707

708 Fig. 6 Variations of bottom O<sub>2</sub> saturation in 2010 (blue) and 2017 (red).



709

710 Fig. 7 Wavelet analysis and the variation of surface  $N_2O$  concentrations (a, b) and surface  $N_2O$  saturations (c,  
 711 d). The dashed red line in (d) indicates the saturation of 100%.



712

713 Fig. 8 Variation of N<sub>2</sub>O flux density at the BE Time Series-Station during 2005–2017. Negative values  
 714 indicated N<sub>2</sub>O influx from the atmosphere and positive values indicated N<sub>2</sub>O efflux to the atmosphere.